

## Article

# Effect of Intensive Abrasion Breakage on Secondary Ball Mills for Magnetite

Chengfang Yuan <sup>1,\*</sup>, Caibin Wu <sup>1,2,\*</sup>, Li Ling <sup>1</sup>, Zheyang Li <sup>1</sup>, Feng Xie <sup>1</sup>, Xin Yao <sup>1</sup> and Yihan Wang <sup>1</sup>

<sup>1</sup> Jiangxi Key Laboratory of Mining Engineering, Jiangxi University of Science and Technology, Ganzhou 341000, China

<sup>2</sup> School of Resources and Environmental Engineering, Jiangxi University of Science and Technology, Ganzhou 341000, China

\* Correspondence: 15779000805@163.com (C.Y.); caibin.wu@jxust.edu.cn (C.W.); Tel.: +86-13970145667 (C.W.)

**Abstract:** In order to investigate the breakage behavior of the feed in industrial secondary ball mills, the breakage characteristics of fine magnetite were analyzed. Magnetite particle breakage produces a bimodal particle size distribution that is consistent with the typical breakage characteristics of abrasion. The secondary ball mill can increase the surface area by reducing the diameter of steel balls to enhance the abrasion. Industrial application results show that after the abrasion of the secondary ball mill for grinding magnetite was enhanced, the circulating load of the grinding-classification system dropped by 29.90% and the specific energy of the secondary ball mill decreased by 39.14%. At the same time, the consumption of steel balls also dropped from 0.17 kg/t to 0.13 kg/t, a decrease of up to 20%. It should be noted that the reduction in the ball diameter should follow certain rules because if the energy of a single collision is lower than the critical breaking energy of the particles, the grinding process will be affected and thus have counterproductive effects.

**Keywords:** magnetite; industrial application; circulating load; specific size energy; energy saving



**Citation:** Yuan, C.; Wu, C.; Ling, L.; Li, Z.; Xie, F.; Yao, X.; Wang, Y. Effect of Intensive Abrasion Breakage on Secondary Ball Mills for Magnetite. *Minerals* **2023**, *13*, 713. <https://doi.org/10.3390/min13060713>

Academic Editors: Josep Oliva and Hernán Anticoi

Received: 28 April 2023

Revised: 20 May 2023

Accepted: 21 May 2023

Published: 23 May 2023



**Copyright:** © 2023 by the authors. Licensee MDPI, Basel, Switzerland. This article is an open access article distributed under the terms and conditions of the Creative Commons Attribution (CC BY) license (<https://creativecommons.org/licenses/by/4.0/>).

## 1. Introduction

Iron resources are the power source of human life and social progress today and the foundation and pillar industry of the world's economic development, and they play an irreplaceable role in life production (a large role with respect to our daily travel using airplanes, cars, and other transportation, and a small role with respect to our cell phones in the chip, which cannot be separated from iron resources). In the development of iron resources, mining and the separation of ore raw materials are essential and very important production links, while the iron ore separation operation, which involves crushing and grinding, is the first process of mineral processing. The grinding operation refers to the process of reducing the particle size of the material in the grinding equipment with the help of grinding media, such as steel balls, porcelain balls, steel rods, and gravel, and the ore itself for impact and grinding action. Grinding consumes the most energy in a mineral-processing plant, with energy consumption accounting for 60% of the total [1]. The primary purpose of grinding is to liberate the target minerals from the gangue minerals sufficiently and monolithically. However, due to the difference in fracture properties between target and gauge minerals, the target mineral often experiences underground or overground pressure, which affects the subsequent mineral separation operations [2]. Therefore, the breakage characteristics of minerals are pivotal for their separation [3–5]. Because the grinding process of magnetite is usually rough, its grinding products have poor particle size characteristics and a low separation index [6–8]. To date, there are a large number of studies on the industrial primary ball mill concerning the grinding characteristic of coarse magnetite [9–11], but there are almost no studies on industrial secondary ball mill regarding fine magnetite.

Most of the research on industrial ball mills has been about their particle-size-prediction models. As early as in the 1970s and 1980s, industrial scale-up models [12] were proposed by experts on the basis of laboratory particle-size-prediction models [13–15]. In this century, Mulenga, a professor at the University of South Africa, invested a lot of effort [16–18] into optimizing Austin’s proposed ball mill scale-up model [19]. Several authors [20–22] have recognized that the product of grinding is produced by the combined effort of three basic size-reduction mechanisms. They are impact, characterized by short time and strong force; cleavage, characterized by a long period of time and strong force; and abrasion, characterized by tangential stress, which will be introduced in detail in Section 2.1. For different particle sizes and states of the ball mill, the breakage characteristics that play a major role in grinding are different. In this paper, the secondary ball mill classification system of Zhangzhuang iron in China will be used as an example to illustrate the improvement of grinding effect by the directional enhancement of crushing. In the research on the breakage characteristics of magnetite, we analyze the main fragmentation mode of magnetite in two-stage mills and enhance it, to achieve the purpose of reducing circulating load and energy saving.

## 2. Theoretical Background

### 2.1. Breakage Characteristics

Material crushing is carried out under the action of mechanical forces; crushing machinery is not just a force to complete the crushing process. The direction and intensity of the stresses that act on the mineral particles affect the breakage characteristics. The three main breakage mechanisms shown in Figure 1 have been identified in the comminution process [20–22]:

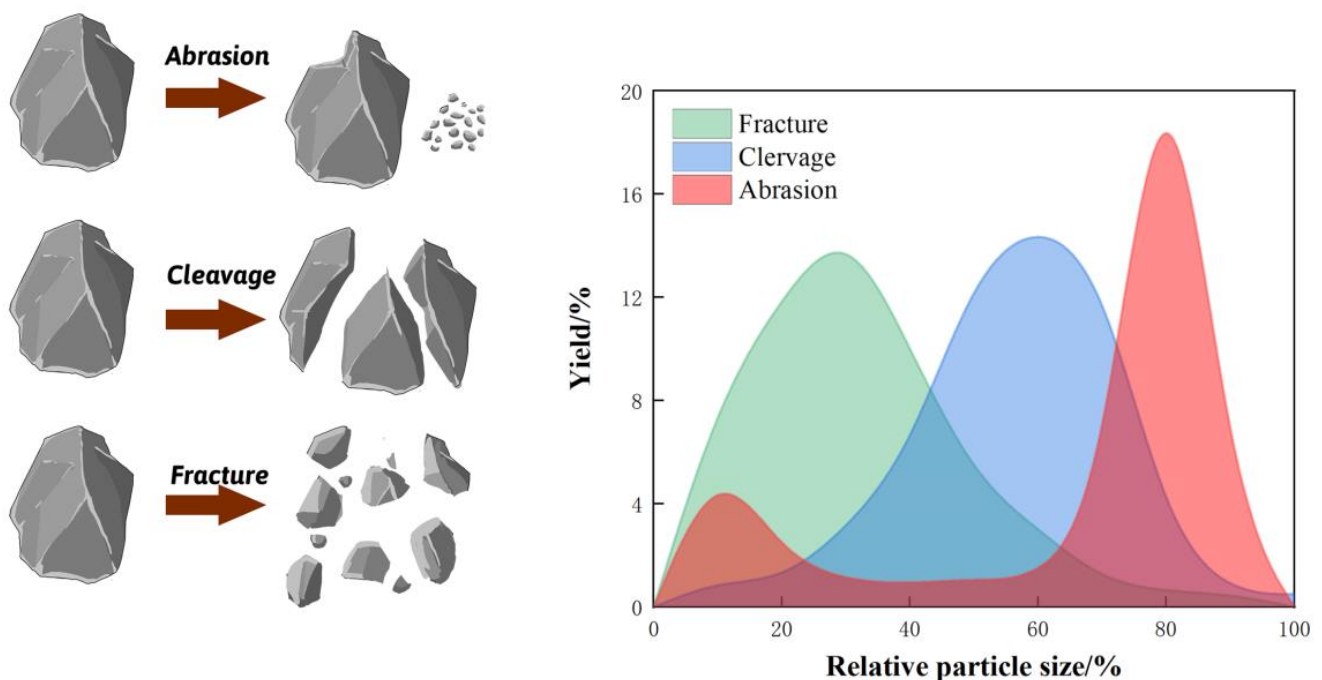


Figure 1. Breakage characteristics of minerals adopted from [22].

**Abrasion:** When the breakage of minerals is acted on by shear stress, particle breakage produces a bimodal particle size distribution consisting of fine particles flaking out of the initial particle surface and particles close to the initial particle size.

**Cleavage:** When the breakage of the particles is caused by the slow action of strong stress, the particle size distribution is single-peaked, which produces fragments 50%–80% smaller than the initial particles.

Fracture: When the breakage of the particles is induced by the rapid action of strong stress, the particle size distribution is single-peaked, producing fragments 20%–70% smaller than the initial particles.

For a certain kind of crushing equipment, in most cases, one kind of force application method is the main method; the other two are complementary, and several kinds of force-application methods exist at the same time to help improve the crushing efficiency. For the grinding operation in mineral processing, the general ore is composed of a variety of minerals, and the physical and mechanical properties of each mineral vary greatly. When the ore is crushed, only the directional strengthening of the main crushing effect can effectively enhance the effectiveness and efficiency of crushing.

## 2.2. Circulating Load

Hydraulic classification is the process of dividing a broad particle size class into a number of narrow-size-class products according to the different settling velocities of the frame in the moving medium under centrifugal and drag forces. Circulating load is an important index of the grinding and classifying system, which can directly reflect the instantaneous processing capacity of ball mills.

Because the ball mill does not have the ability to classify according to the size, the grinding product of the open circuit has more coarse minerals that are not conducive to subsequent separation [23]. To solve this problem, ball mills are often used in conjunction with classifying equipment. The discharge of the ball mill enters the classifier, which returns the coarse particles (underflow) to the ball mill for regrinding, and the fine particles (overflow) are the final product. In practice, the grinding system in which the ball mill cooperates with the classifier and returns the unqualified coarse products to the ball mill for re-crushing is called the closed circuit grinding system. A grinding system in which the crushed product is not classified or returned to the ball mill is called an open-circuit grinding system. Therefore, the circulating load is a crucial parameter to evaluate the running state of the grinding mill. For the secondary ball mill, a common grinding-classification system is shown in Figure 2.

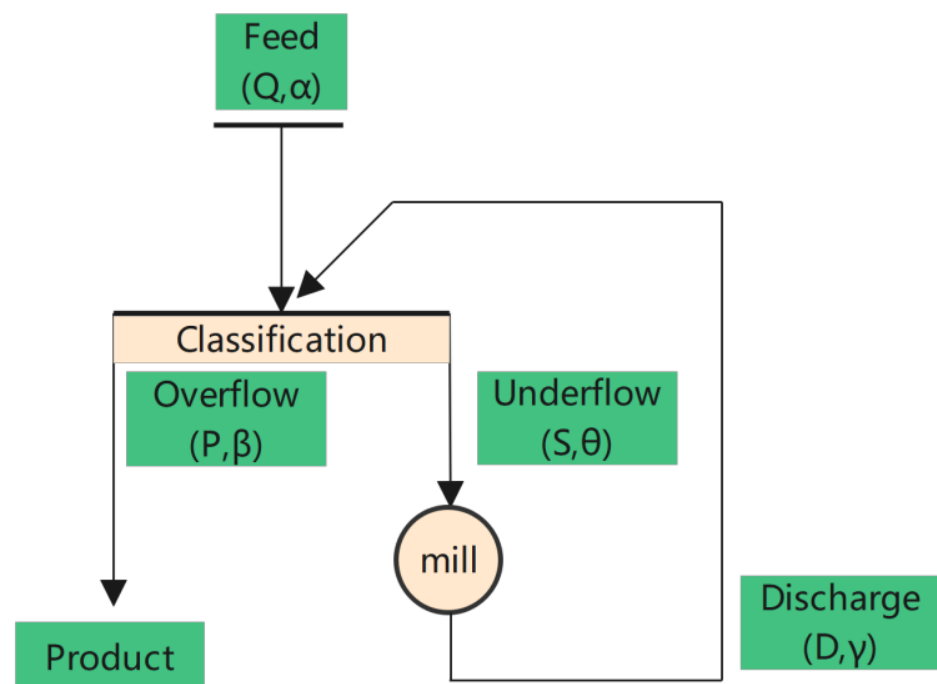


Figure 2. Common grinding-classification system of the secondary ball mill.

According to its definition, circulating load can be derived as:

$$Q + S = Q + CQ = Q(1 + C) \quad (1)$$

where  $C$  represents the circulating load (%) of the grinding mill,  $S$  is the underflow discharge (mass) of the classifier, and  $Q$  represents the fresh feed (mass) entering the grinding system. However, the mass of the slurry in industry is difficult to measure, so it is difficult to calculate the circulating load using Equation (1). The calculation of the circulating load is usually combined with the conservation of mass for the whole process and for a specific particle size:

$$Q + D = P + S \quad (2)$$

$$Q\alpha + D\gamma = P\beta + S\theta \quad (3)$$

where  $\alpha$ ,  $\beta$ ,  $\theta$ , and  $\gamma$  represent the proportion of specific size of various products, respectively. The common circulating load calculation formula can be derived by combining Equations (2) and (3):

$$C = \frac{\beta - \alpha}{\gamma - \theta} \quad (4)$$

### 2.3. Specific Size Energy

The energy utilization efficiency of ball mills is a very important indicator, which reflects the percentage of useful energy. The amount of energy required to produce a qualified particle size ( $\sim 75 \mu\text{m}$ ) per unit mass is called specific size energy (SSE), which is calculated according to the newly generated particles, energy consumption, and throughput [24,25], as shown in the following equations:

$$\text{Specific energy} = SE = \frac{P}{Q} \quad (5)$$

$$\text{Specific size energy} = SSE = \frac{SE}{\gamma - \theta} \quad (6)$$

where  $P$  represents the grinding energy consumption of the mill;  $Q$  is the throughput of the grinding mill; and  $\gamma$  and  $\theta$  represent the percentage of  $\sim 75 \mu\text{m}$  in grinding feed and grinding discharge, respectively.

## 3. Materials and Methods

### 3.1. Materials

The magnetite used in this study was the fresh feed of the secondary ball mill, which came from Zhangzhuang iron in Huoqiu, Anhui Province, China. The bulk density of the magnetite, measured by the water replacement method, was  $2.98 \text{ t/m}^3$ . The feed size characteristics of the secondary ball mill are shown in Table 1, the main compound composition characteristics are shown in Table 2, and the mineral form and content of Fe are shown in Table 3. The iron content of the fresh feed ore is as high as 82.83%, indicating that the purity of the iron ore is already high. In addition to Fe, the content of silica is 12.98%, indicating that the main vein stone mineral in the fresh feed ore is quartz. The iron physical phase analysis of the fresh feed ore shows that magnetite accounts for 86.18%, followed by hematite, accounting for 3.59%. The feed had already gone through a magnetic separation operation, so its iron content was high, and the magnetite accounted for a relatively large proportion. From the particle size characteristics of the feed ore, it can be seen that the iron grade increases as the particle size decreases, indicating that magnetite is distributed in this iron ore with a fine particle size, which requires a high degree of monomer dissociation to separate and enrich it magnetically.

**Table 1.** The feed size characteristics of the secondary ball mill.

Fractions/mm	Yield/%	Grade (Fe)/%	Iron Content/%
−0.3 + 0.212	3.63	24.46	1.43
−0.212 + 0.15	5.65	22.56	2.05
−0.15 + 0.106	10.79	42.73	7.42
−0.106 + 0.075	23.49	66.75	25.23
−0.075 + 0.045	41.13	70.97	46.97
−0.045 + 0.038	5.04	69.36	5.63
−0.038 + 0.023	5.49	68.44	6.05
−0.023	4.79	67.95	5.24
Total/%	100.00	62.15	100.00

**Table 2.** The main compound composition characteristics of the feed.

Compounds	TFe	SiO <sub>2</sub>	Al <sub>2</sub> O <sub>3</sub>	CaO	MgO
Content/%	82.83	12.98	1.06	0.71	0.81

**Table 3.** The mineral form and content of Fe in the feed.

Minerals	Magnetite	Hematite	Magnetic Pyrite	Pyrite	Carbonate Iron	Silicate Iron
Content/%	86.18	3.59	0.11	0.80	2.24	6.08

### 3.2. Process Flow

Zhangzhuang iron ore mine is a typical magnetite mining unit in China, with an annual processing capacity of 3 million tons. The crushing operation is a typical three-stage, one-closed circuit crushing process, and the product after fine crushing goes to the high-pressure rollers for re-processing; finally, the −3 mm magnetite ore is obtained to enter the grinding and classification operation. As shown in Figure 3, the grinding and classifying system of Zhangzhuang iron is a traditional two-stage with a closed circuit; the primary mill is MQY4060 and the secondary ball mill is MYS4060, whose parameters are shown in Table 4, with the classification equipment of both grinding stages being hydrocyclone. Hydrocyclone is gravity classification equipment; compared with the high-frequency screen, it has larger capacity and does not require frequent screen replacement, so most magnetite-ore-processing plants use hydrocyclone as classification equipment. During the process, the fresh feed went into the primary ball mill, the discharge of which entered the primary hydrocyclone. The overflow of the primary hydrocyclone went into the secondary hydrocyclone, and the underflow returned to the primary ball mill. In the secondary hydrocyclone, its overflow became the final product, and its underflow went back to the secondary ball mill.

**Table 4.** The specific parameters of the secondary mill.

Mill Conditions						Grinding Media		
Throughput	Type	Diameter	Length	Linear	Rotational Speed Ratio	Type	Diameter	Ball Filling
220 ± 10	Overflow	4.0 m	6.0 m	Magnetic liner	72%	Steel ball	50 mm	42% ± 1%

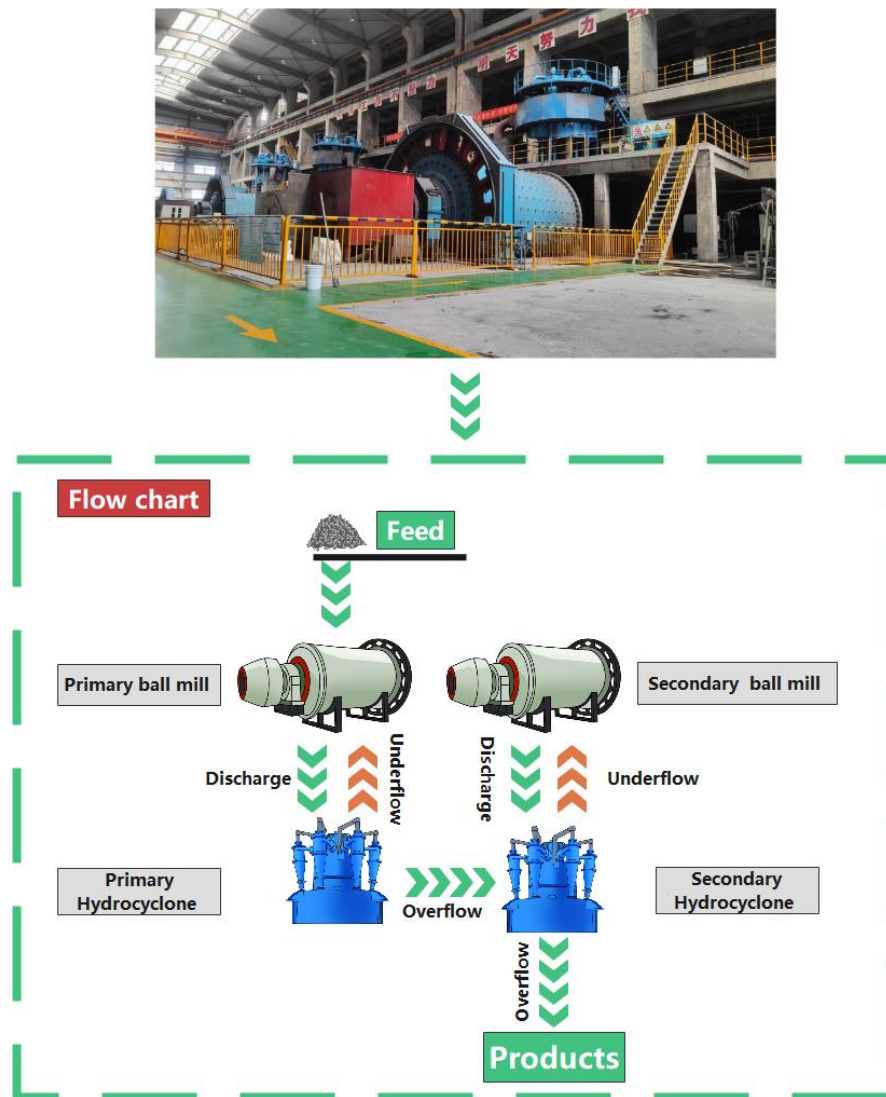


Figure 3. Grinding flow chart of Zhangzhuang iron.

### 3.3. Breakage Characteristics

In order to derive the main breakage characteristic of the fresh feed, narrow-size-batch grinding experiments were carried out in the laboratory. The tests were carried out in an XBM ball mill with a speed of 86 r/min and a cylinder volume of 2.5 L ( $D \times L = 140 \text{ mm} \times 160 \text{ mm}$ ). The amount of ore fed into the mill for each experiment was 200 g, and the mass concentration of the mill was 67%, both of which were constant parameters. The diameter of the steel balls is 18 mm, and the filling rate is 30%, and all of the products after grinding are sieved using a standard set of screens. The feed was classified using a sieve shaker, and the fractions of feeds for the experiment were  $-0.600 + 0.425 \text{ mm}$ ,  $-0.425 + 0.300 \text{ mm}$ ,  $-0.300 + 0.212 \text{ mm}$ ,  $-0.212 + 0.150 \text{ mm}$ , and  $-0.150 + 0.106 \text{ mm}$ . Figure 4 shows the variation in the yield of daughter fractions for each feed fraction at different grinding times. The breakage characteristics of the Feed fra.1 ( $-0.600 + 0.425 \text{ mm}$ ) showed a clear bimodal particle size distribution, and the yields of Daughter fra.1 (the coarsest fraction) and fra.9 (the finest fraction) were significantly higher than those of other subclasses. With the increase in grinding time, the yield of Daughter fra.1 gradually decreased and Daughter fra.9 increased, which was consistent with the abrasion-breakage behavior. The other four feed fractions also showed this phenomenon, indicating that for magnetite of  $-600 + 0.106 \text{ mm}$ , which was the particle size range of the feed of the

industrial secondary ball mill, the stress used for breakage was shear stress, conforming to the breakage characteristics of abrasion.

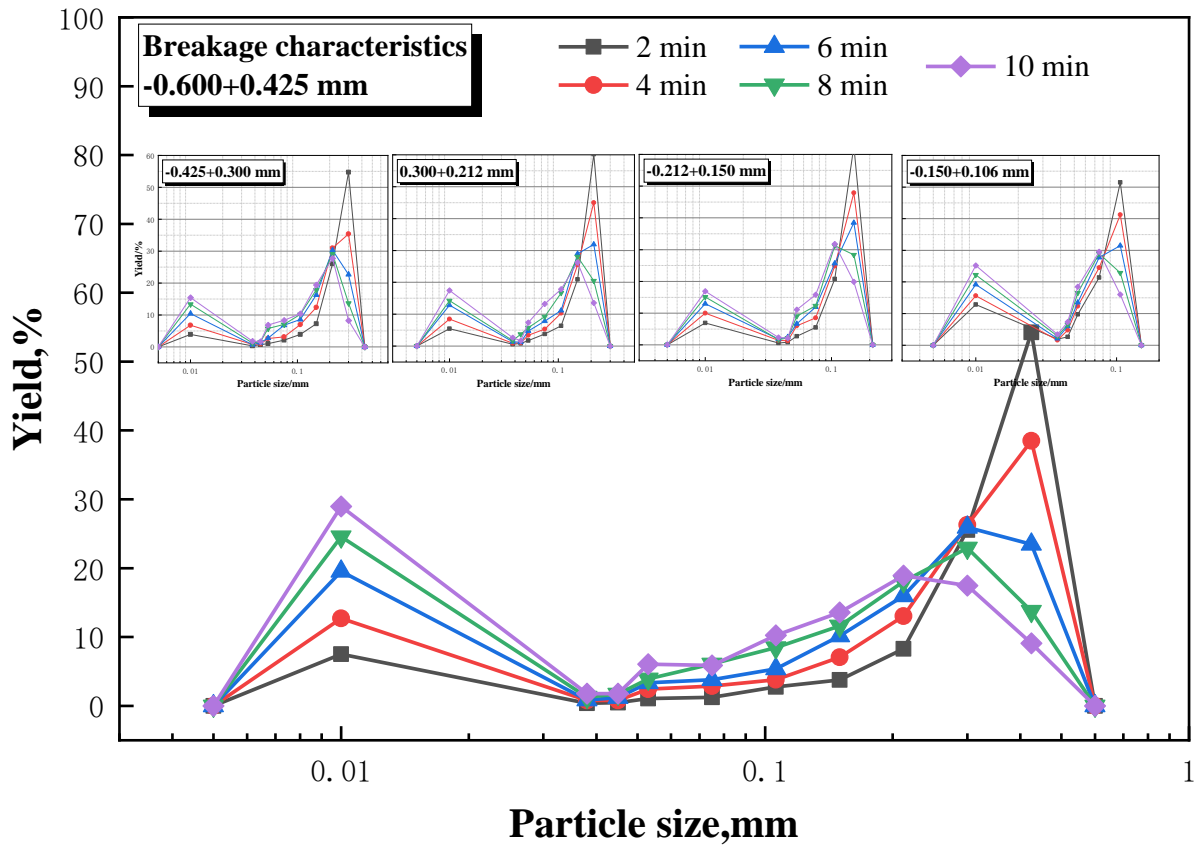


Figure 4. The yield of daughter fraction after different grinding time t.

Figure 5 is the SEM result of the discharge grinding for 2 min. Figure 5a shows the image with 100 times magnification; the discharge was mainly divided into two parts: the abraded particles and the abrade-generating particles. In order to identify the fragmentation characteristics instantly, Figure 5b shows the image with 1000 times magnification, and it can be clearly seen that there were obvious abrasion marks on the edge of the particles.

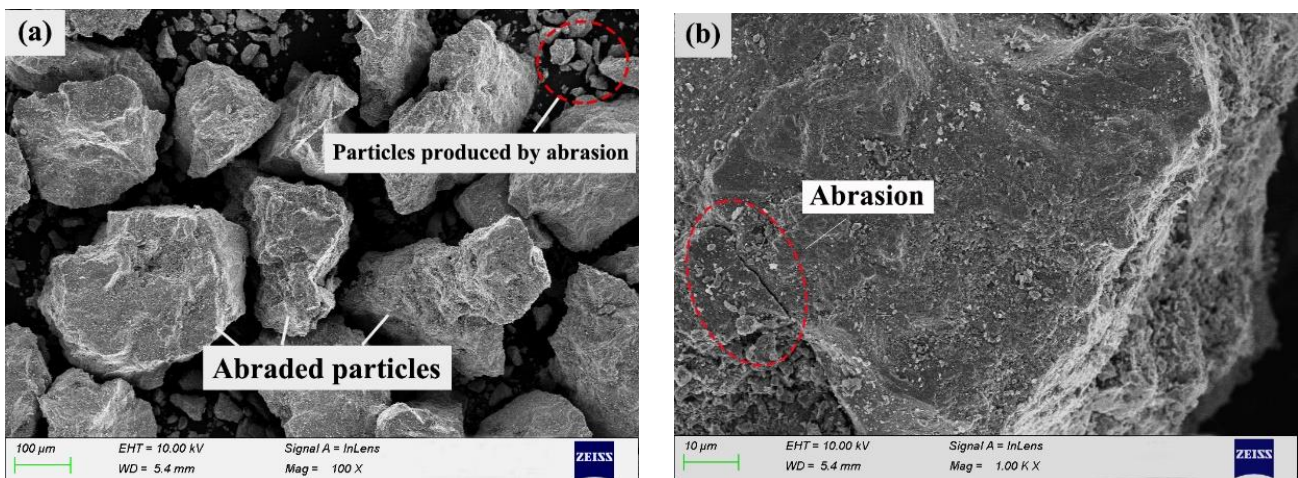


Figure 5. The SEM of the discharge after 2 min of grinding time.

The above results confirm that the main breakage characteristic of the secondary mill for magnetite is abrasion, so it is valuable for the industry to seek a method that can enhance the abrasion. In fact, for the primary grinding operation, the feed size of the ore is larger, the mechanical strength of the individual particles of the ore is greater, and the occurrence of the crushing behavior mainly depends on the collision energy, so for the primary grinding operation to strengthen the impact, crushing can be used to improve the grinding efficiency. For the secondary section grinding operation, the feed size of the ore is small and the ore is easily caught in the gaps between the steel balls and cannot be effectively crushed. The occurrence of crushing behavior mainly depends on the effective collision probability, so for the secondary grinding operation, increasing the specific surface area of the grinding media can improve the grinding efficiency.

### 3.4. Industrial Solutions

The main breakage method for the feed of the secondary ball mill is abrasion, in which with the grinding surface area increases and the probability of abrasion breakage increases, thus improving the grinding effect (retaining the same amount of the newly generated particles with a size less than 0.075 mm after grinding). As shown in Figure 6, with the same total weight, the total surface area of the grinding media can be increased by reducing the size of the steel balls. In other words, with the same grinding effect, the total weight of the balls can be reduced (from 116.4 tons to 93.1 tons) by reducing the diameter (from 50 mm to 40 mm) of the steel balls, which was the theoretical basis of the secondary ball mill energy-saving project of Zhangzhuang iron. Only the diameter and filling rate of the balls vary in industrial applications, while the rest of the parameters remain largely unchanged. The industrial trial went smoothly, and the second stage grinding and classifying system was in stable operation and reached production in only about a week.

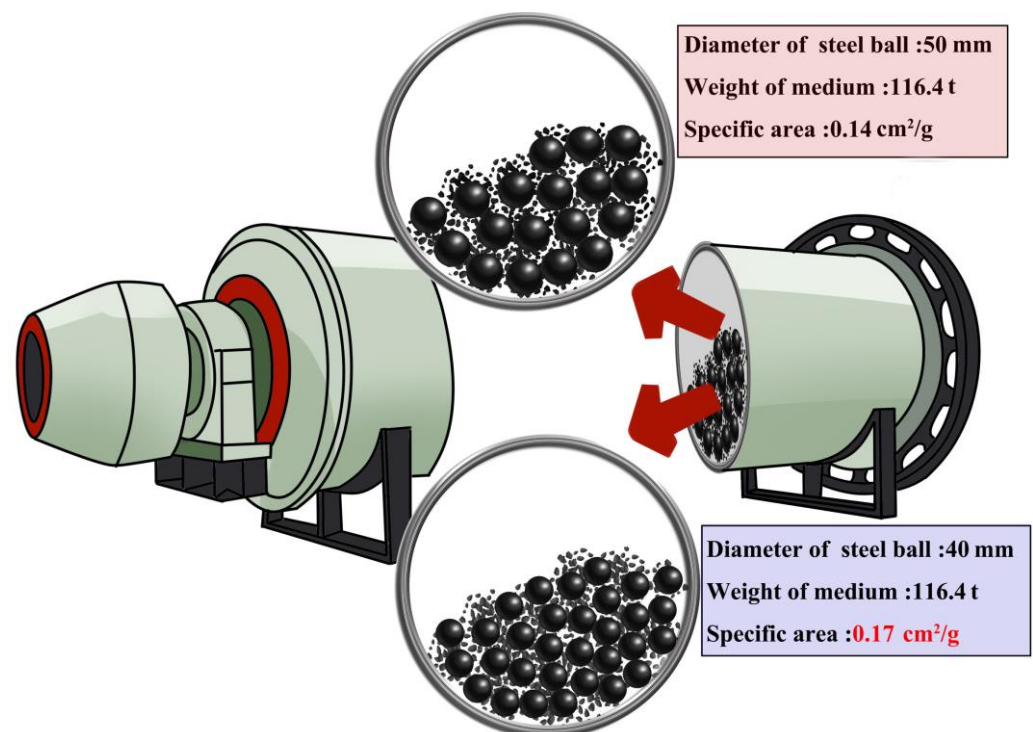


Figure 6. The industrial application schematic.

## 4. Results and Discussion

### 4.1. Particle Size Characteristics and Circulating Load

The main operating parameters of the grinding and classifying system, such as ball mill speed (rotation speed ratio is 72%), hydrocyclone underflow port diameter (60 mm),

cyclone pressure (150 kPa), and grinding mass concentration (75%), were not significantly changed after the adoption of the method of increasing the grinding surface area and thus directionally enhancing the crushing capacity. The improvement of the grinding effect is shown in Figure 7. The newly generated product with a particle size of less than 0.075 mm was 14.38%, which was 4.8 percent higher than before. The fineness of the final product of the grinding and classifying system and the second overflow also increased by 2.14% compared to the previous data. In addition, the Fe occupancy of the fraction overground (−0.023 mm fraction) in discharge was approximately 1% lower than before. The above three points confirmed that the main method of mineral fragmentation in the industrial secondary ball mill is also abrasion, and the grinding effect of ball mills can be enhanced by increasing the surface area of the grinding medium.

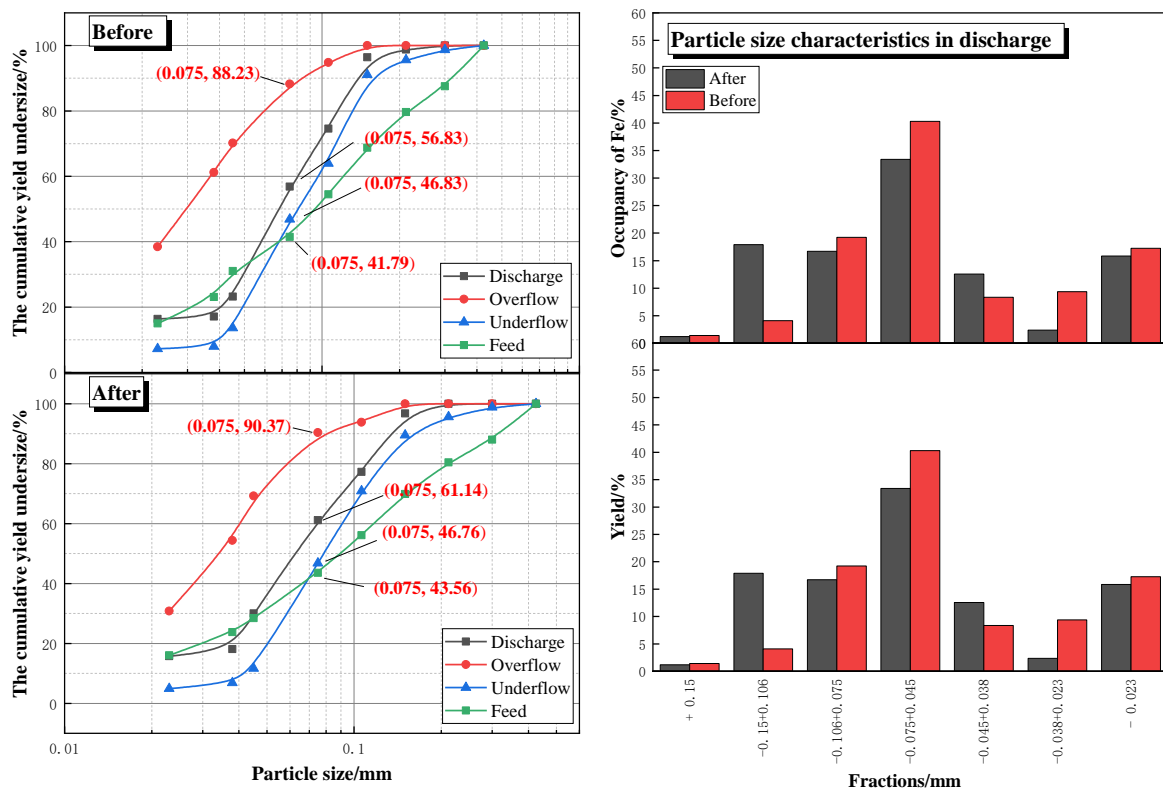


Figure 7. Improvement of grinding effect in the secondary ball mill.

Before industrial application, the −75 μm content in the fresh feed, discharge, overflow, and underflow were 41.79%, 56.83%, 88.23%, and 46.83%, respectively, and the slurry mass concentration was 45.4%, 75.2%, 12.5%, and 79.8%, respectively. Based on the particle size characteristics of the two-stage grinding-classification system, the circulating load  $C_1$  can be calculated as:

$$C_1 = \frac{\beta - \alpha}{\gamma - \theta} = \frac{88.23\% - 41.76\%}{56.83\% - 46.53\%} \times 100\% = 464.40\% \tag{7}$$

Through industrial applications, the −75 μm content in the fresh feed, discharge, overflow, and bottom streams was 43.56%, 61.14%, 90.37% and 46.76%, respectively; the slurry mass concentration was 45.8%, 75.9%, 12.9% and 79.5%, respectively; and the circulating load  $C_2$  can be calculated as:

$$C_2 = \frac{\beta - \alpha}{\gamma - \theta} = \frac{90.37\% - 43.56\%}{61.14\% - 46.76\%} \times 100\% = 325.52\% \tag{8}$$

The circulating load of the grinding and classifying system before industrial application was 464.40%, and the circulating load of the grinding and classifying system after industrial application was 325.52%. Increasing the specific surface area to enhance the abrasion breakage of magnetite in the secondary ball mill can reduce the circulation load of the second stage grinding and classifying system by 138.88 percentage points, a decrease of up to 29.90%. Meanwhile, the increase in the newly generated particles and the decrease in the circulating load also proved that the main breakage characteristic of fine magnetite is abrasion.

#### 4.2. Specific Size Energy

Because the total weight of the media in the secondary ball mill was reduced, the operating current also appeared to drop significantly during the gradual replacement of the steel balls. The variation of the operating current is shown in Figure 8, which was about 80 A at the beginning of the industrial experiment and about 70 A at the later stage of stable production, demonstrating a decrease of 10 A or 12.5%. Combined with the newly generated particles in the previous section, the specific size energy ( $SSE_1$ ) before the industrial application can be derived as:

$$SSE_1 = \frac{SE}{\gamma - \theta} = \frac{800}{220 \times (56.83\% - 46.53\%)} = 36.36 \text{ kWh/t} \quad (9)$$

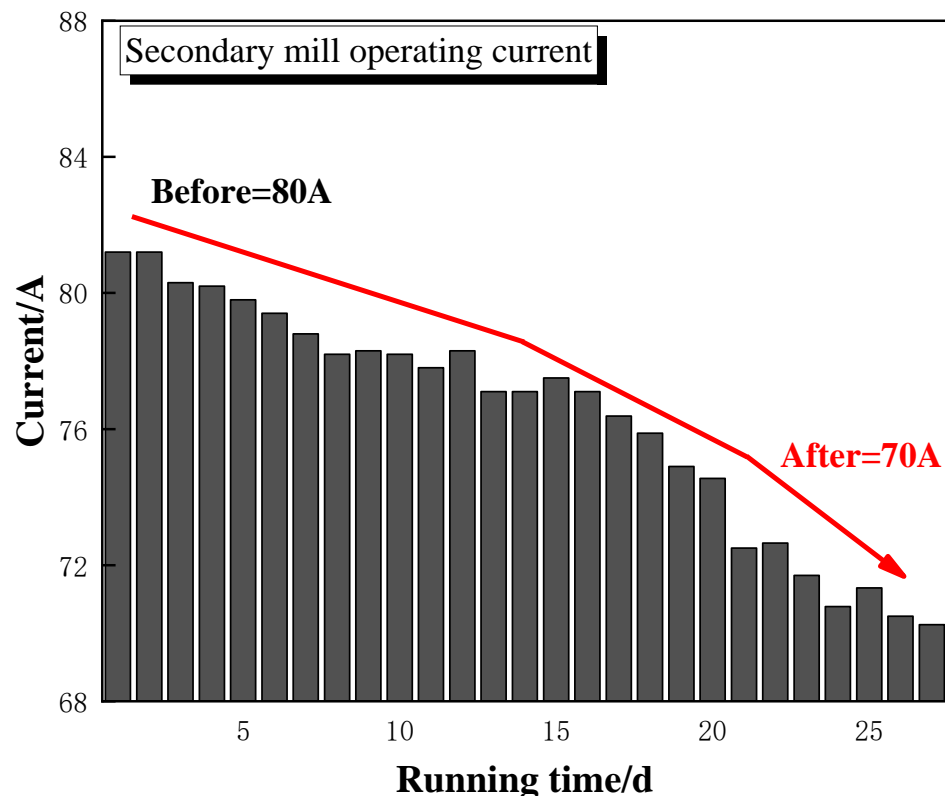


Figure 8. Change in the operating current of the secondary ball mill.

Through industrial applications, the specific size energy ( $SSE_2$ ) can be calculated as:

$$SSE_2 = \frac{SE}{\gamma - \theta} = \frac{700}{220 \times (61.14\% - 46.76\%)} = 22.13 \text{ kWh/t} \quad (10)$$

The specific size energy of the grinding and classifying system before industrial application was 36.36 kWh/t, and the specific size energy of the grinding and classifying system after industrial application was 22.13 kWh/t. Increasing the specific surface area

to enhance the abrasion breakage of magnetite in the secondary ball mill can reduce the total weight of the loaded balls while improving the operation of the two-stage grinding-classification system, which results in a significant increase in energy utilization efficiency. After industrial application, the specific size energy of the second stage mill decreased by 14.23 percentage points, a decline of up to 39.14%.

According to the energy consumption conversion, the energy-saving optimization of the secondary ball mill of Zhangzhuang iron can save 2 million kWh of electricity per year. Given that 0.32 kg of standard coal is needed to produce one unit of electricity, it can save about 640 tons of standard coal and reduce the release of 170 tons of carbon dioxide per year.

When the ball diameter of the steel ball is reduced, the monolithic mass is then reduced in square steps. The monolithic mass is reduced, and the instantaneous energy of steel ball collision is also sharply reduced, so the theoretical consumption of steel balls is also reduced. The daily processing capacity of the Zhangzhuang iron processing plant is 10,000 t of magnetite ore; 50 t of steel balls need to be replenished in one month before the industrial test, and the ball consumption of steel balls is 0.17 kg/t. After the industrial test, only 40 t of steel balls need to be replenished in one month, and the ball consumption of steel balls is 0.13 kg/t, which is 20% lower than before the industrial test.

## 5. Conclusions

The breakage characteristics of fine magnetite were analyzed to investigate the breakage behavior of the feed in industrial secondary ball mill. Through the study of the breakage characteristics of the five feed fractions, it was found that particle breakage produces a bimodal particle size distribution consisting of fine particles flaking out of the initial particle surface and particles close to the initial particle size, which is consistent with the typical breakage characteristics of abrasion.

In industrial applications, the secondary ball mill can increase the surface area by reducing the diameter of steel balls to enhance the abrasion, so that it can have a similar grinding effect with lower total media weight, thus achieving the purpose of lower circulating load and higher energy utilization efficiency. The industrial application results show that after the enhanced abrasion of the secondary ball mill was achieved for magnetite, the circulating load of the grinding-classification system fell by 29.90% and the specific energy (SSE) of the secondary ball mill tumbled by 39.14%. At the same time, the reduced ball diameter reduces the collision energy, which in turn strongly reduces the consumption of steel balls by 20% compared to the consumption of steel balls before the industrial test.

For the secondary section grinding operation, the feed size of the ore is small and the ore is easily caught in the gaps between the steel balls and cannot be effectively crushed. The occurrence of crushing behavior mainly depends on the effective collision probability, so for the secondary grinding operation increasing the specific surface area of the grinding media can improve the grinding efficiency. This method is suitable for all conventional secondary ball mills for grinding magnetite. However, given that the grinding process will be influenced and produce counterproductive effects when the energy of a single collision is lower than the critical breaking energy of the particles, the ball diameter should not be reduced at liberty.

**Author Contributions:** Methodology, L.L.; software, Z.L.; investigation, F.X.; resources, Y.W.; data curation, X.Y.; writing—review and editing, C.Y.; and supervision, C.W. All authors have read and agreed to the published version of the manuscript.

**Funding:** This research was funded by National Natural Science Foundation of China: 51764015.

**Acknowledgments:** The authors gratefully acknowledge the financial support from the National Natural Science Foundation of China (No. 51764015).

**Conflicts of Interest:** The authors declare no conflict of interest.

## References

1. Norgate, T.; Haque, N. Energy and greenhouse gas impacts of mining and mineral processing operations. *J. Clean. Prod.* **2010**, *18*, 266–274. [[CrossRef](#)]
2. Guo, W.; Han, Y.; Li, Y.; Tang, Z. Impact of ball filling rate and stirrer tip speed on milling iron ore by wet stirred mill: Analysis and prediction of the particle size distribution. *Powder Technol.* **2021**, *378*, 12–18. [[CrossRef](#)]
3. Gupta, V.K. Effect of particulate environment on the grinding kinetics of mixtures of minerals in ball mills. *Powder Technol.* **2020**, *375*, 549–558. [[CrossRef](#)]
4. Gupta, V.K. Energy absorption and specific breakage rate of particles under different operating conditions in dry ball milling. *Powder Technol.* **2020**, *361*, 827–835. [[CrossRef](#)]
5. Chimwani, N.; Glasser, D.; Hildebrandt, D.; Metzger, M.J.; Mulenga, F.K. Determination of the milling parameters of a platinum group minerals ore to optimize product size distribution for flotation purposes. *Miner. Eng.* **2013**, *43–44*, 67–78. [[CrossRef](#)]
6. Zhang, X.; Han, Y.; Gao, P.; Li, Y. Effects of grinding media on grinding products and flotation performance of chalcopyrite. *Miner. Eng.* **2020**, *145*, 106070. [[CrossRef](#)]
7. Liao, N.; Wu, C.; Xu, J.; Feng, B.; Wu, J.; Gong, Y. Effect of Grinding Media on Grinding-Flotation Behavior of Chalcopyrite and Pyrite. *Front. Mater.* **2020**, *7*, 176. [[CrossRef](#)]
8. Lan, J.; Dong, Y.; Xiang, Y.; Zhang, S.; Mei, T.; Hou, H. Selective recovery of manganese from electrolytic manganese residue by using water as extractant under mechanochemical ball grinding: Mechanism and kinetics. *J. Hazard. Mater.* **2021**, *415*, 125556. [[CrossRef](#)]
9. Javad Koleini, S.M.; Barani, K.; Rezaei, B. The Effect of Microwave Treatment on Dry Grinding Kinetics of Iron Ore. *Miner. Process. Extr. Metall. Rev.* **2012**, *33*, 159–169. [[CrossRef](#)]
10. Sen, S. Grinding of magnetite using a waterjet driven cavitation cell. *Powder Technol.* **2016**, *297*, 34–43. [[CrossRef](#)]
11. Si, L.; Cao, Y.; Fan, G.; Gao, M. The Effect of Grinding Media on Mineral Breakage Properties of Magnetite Ores. *Geofluids* **2021**, *2021*, 1575886. [[CrossRef](#)]
12. Herbst, J.A. Scale-up procedure for continuous grinding mill design using population balance models. *Int. J. Miner. Process.* **1980**, *7*, 1–31. [[CrossRef](#)]
13. Kesall, D.F. Continuous Grinding in a Small Wet Ball Mill Part II. A Study of the Influence of Hold-Up Weight. *Powder Technol.* **1968**, *69*, 162–168.
14. Kesall, D.F. Continuous Grinding in a Small Wet Ball Mill Part I. A Study of influence of Ball Diameter. *Powder Technol.* **1968**, *68*, 291–300. [[CrossRef](#)]
15. Kesall, D.F. Continuous Grinding in a Small Wet Ball Mill. Part III. A Study of Distribution of Residence Time. *Powder Technol.* **1969**, *70*, 170–178. [[CrossRef](#)]
16. Mulenga, F.K. Sensitivity analysis of Austin's scale-up model for tumbling ball mills—Part 1. Effects of batch grinding parameters. *Powder Technol.* **2017**, *311*, 398–407. [[CrossRef](#)]
17. Mulenga, F.K. Sensitivity analysis of Austin's scale-up model for tumbling ball mills—Part 2. Effects of full-scale milling parameters. *Powder Technol.* **2017**, *317*, 6–12. [[CrossRef](#)]
18. Mulenga, F.K. Sensitivity analysis of Austin's scale-up model for tumbling ball mills—Part 3. A global study using the Monte Carlo paradigm. *Powder Technol.* **2017**, *322*, 195–201. [[CrossRef](#)]
19. Austin, L.G. A Review: Introduction to the Mathematical Description of Grinding as a Rate Process. *Powder Technol.* **1971**, *5*, 1–17. [[CrossRef](#)]
20. Menacho, J.M. Some Solutions for the Kinetics of Combined Fracture and Abrasion Breakage. *Powder Technol.* **1986**, *49*, 87–96. [[CrossRef](#)]
21. Hornung, U. Diffusion Models for Fractured Media. *J. Math. Anal. Appl.* **1990**, *147*, 69–80. [[CrossRef](#)]
22. Hennart, S.L.A.; Wildeboer, W.J.; van Hee, P.; Meesters, G.M.H. Identification of the grinding mechanisms and their origin in a stirred ball mill using population balances. *Chem. Eng. Sci.* **2009**, *64*, 4123–4130. [[CrossRef](#)]
23. Jankovic, A.; Valery, W. Closed circuit ball mill—Basics revisited. *Miner. Eng.* **2013**, *43–44*, 148–153. [[CrossRef](#)]
24. Guo, W.; Han, Y.; Gao, P.; Li, Y.; Tang, Z. Effect of feed size on residence time and energy consumption in a stirred mill: An attainable region method. *Powder Technol.* **2021**, *379*, 485–493. [[CrossRef](#)]
25. Fang, X.; Wu, C.; Yuan, C.; Liao, N.; Chen, Z.; Li, Y.; Lai, J.; Zhang, Z. Can ceramic balls and steel balls be combined in an industrial tumbling mill? *Powder Technol.* **2022**, *412*, 118020. [[CrossRef](#)]

**Disclaimer/Publisher's Note:** The statements, opinions and data contained in all publications are solely those of the individual author(s) and contributor(s) and not of MDPI and/or the editor(s). MDPI and/or the editor(s) disclaim responsibility for any injury to people or property resulting from any ideas, methods, instructions or products referred to in the content.